Article

pubs.acs.org/Biomac

Solid-State ^{13}C NMR Delineates the Architectural Design of Biopolymers in Native and Genetically Altered Tomato Fruit Cuticles

Subhasish Chatterjee,[†] Antonio J. Matas,[‡,§] Tal Isaacson,[‡,∥] Cindie Kehlet,[⊥] Jocelyn K.C. Rose,[‡] and Ruth E. Stark*[,†]

[†]Department of Chemistry and Biochemistry, The City College of New York, City University of New York Graduate Center Ph.D. Programs in Biochemistry and Chemistry and CUNY Institute for Macromolecular Assemblies, New York, New York 10031, United States

[‡]Plant Biology Section, School of Integrative Plant Science, Cornell University, Ithaca, New York 14853, United States

[⊥]Department of Mathematics and Science, Pratt Institute, Brooklyn, New York 11205, United States

Supporting Information

ABSTRACT: Plant cuticles on outer fruit and leaf surfaces are natural macromolecular composites of waxes and polyesters that ensure mechanical integrity and mitigate environmental challenges. They also provide renewable raw materials for cosmetics, packaging, and coatings. To delineate the structural framework and flexibility underlying the versatile functions of cutin biopolymers associated with polysaccharide-rich cell-wall matrices, solid-state NMR spectra and spin relaxation times were measured in a tomato fruit model system, including different developmental stages and surface phenotypes. The hydrophilic−hydrophobic balance of the cutin ensures compatibility with the underlying polysaccharide cell walls; the hydroxy fatty acid structures of outer epidermal cutin also support deposition of hydrophobic waxes and aromatic moieties while promoting the formation of cell-wall cross-links that rigidify and strengthen the cuticle composite during fruit development. Fruit cutin-deficient tomato mutants with compromised microbial resistance exhibit less efficient local and collective biopolymer motions, stiffening their cuticular surfaces and increasing their susceptibility to fracture.

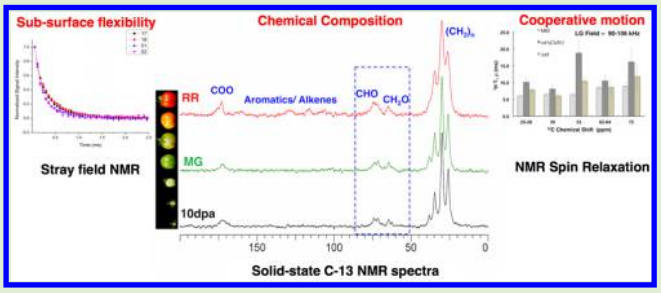

INTRODUCTION

Environmental interactions in the nonwoody aerial organs of terrestrial plants are influenced by protective cuticles that consist of hydrophobic waxes and insoluble cutin polymers assembled on the outer face of epidermal cell walls.[1] These natural composite materials possess lipid constituents with common characteristics, ester-linked architectures, and biosynthetic origins.[2,3] Analogously to suberin polyesters that accumulate predominantly in the extracellular environment of specific root tissues,[4,5] cutins can offer renewable sources of industrially useful ω-hydroxy fatty acids that can be engineered to form low-melting cross-linked semicrystalline polyesters with desirable hydrophobic properties, fiber-forming capabilities, and biodegradability.[6] Moreover, the (macro)molecular organization underlying the waterproofing and antimicrobial capabilities of plant cuticles can delineate design strategies for water-resistant paints, coatings, or textiles.[7]

The tomato (*Solanum lycopersicum*) fruit has emerged as an excellent model for the study of protective cuticular membranes: its relatively thick cuticle is poreless, uniform, and comparatively easy to isolate; recently available genomic information also opens the way for biosynthetic engineering of its polymeric cuticular constituents.[8−12] These favorable attributes are exemplified by the recent description of cuticles on the inner and outer epidermal surfaces of the fruit pericarp ("flesh"),[13] for which considerable progress has been made in identifying the genes and enzymes responsible for ester formation[9,14,15] and the nonenzymatic assembly processes that could occur additionally during formation of the cutin biopolymer.[16−18] The tomato fruit cuticle also represents a natural membrane material for which measurements of permeability, microbial resistance, and mechanical stiffness have been reported.[8]

In the current work, solid-state nuclear magnetic resonance (NMR) spectra and flexibility measurements were used to link site-specific molecular characteristics of tomato fruit cuticles with their capabilities for cross-linking and environmental interactions, their potential resistance to cracking, and their stages of development and ripening. We address the following questions: (1) how the inner and outer epidermal cuticles of the fruit develop structurally during ripening in ways that could reflect their contrasting waterproofing and strengthening functions; (2) which distinctive attributes of chemical composition and molecular flexibility in the cuticular materials

Received: October 1, 2015
Revised: December 8, 2015
Published: December 10, 2015

DOI: 10.1021/acs.biomac.5b01321
Biomacromolecules 2016, 17, 215−224

are associated with anomalous phenotypes in a library of single-gene tomato mutants; (3) which design principles for environmental protection in macromolecular assemblies[19] emerge from studies of molecular structure and flexibility using the tomato fruit cuticle as a model biopolymer system.

EXPERIMENTAL SECTION

Plant Material. Tomato (*S. lycopersicum* cv Ailsa Craig and cv M82) plants were grown in a greenhouse in Ithaca, NY, as described previously,[8,13] and fruits were harvested at three developmental stages: 10 days post-anthesis (10-DPA), mature green (full size, MG), and red ripe (full size, 4−5 days past color break, RR). Mutated tomato lines obtained from the "Genes that Make Tomatoes" germplasm collection (http://zamir.sgn.cornell.edu/mutants) included e4247m1 (first named *cutin deficient 1 [cd1]*,[14] the mutated gene of which was later renamed *cutin synthase like 1 [CUS1]*),[15] e4393m2 *(cutin deficient 2 [cd2])*, and n3056m1 *(cutin deficient 3 [cd3]*, the causal mutation of which is the cytochrome P450 gene SlCYP86A69).[20] Naming conventions based on the phenotype or mutated gene have been described previously,[8,13,14] and we designate the three mutants considered together as *cd(n)*. Outer epidermal cuticles from red ripe fruit of M82 and *cd(n)* mutants were isolated enzymatically using a standard cellulase-pectinase cocktail for 7−10 days to cleave polysaccharide cell-wall bonds and remove the resulting sugar moieties.[8,13,21] For comparative studies of inner epidermal (iep) and outer epidermal (oep) Ailsa Craig cuticles,[13] enzymatic incubations were conducted for up to 4 months without shaking to avoid sample fragmentation; the oep was removed manually with a razor before sectioning the pericarp to obtain the iep, and each tissue portion was incubated separately with cell wall-degrading enzymes. For both sets of samples, exhaustive dewaxing to isolate the cutin biopolymer was accomplished by successive overnight Soxhlet extractions under reflux conditions using ACS grade methanol, chloroform, and hexanes.[22,23]

Solid-State Nuclear Magnetic Resonance Spectroscopy. ^{13}C solid-state NMR measurements of average or "bulk" properties were conducted on 2−5 mg of exhaustively dewaxed cuticular material at magic-angle spinning (MAS) rates of 10 or 15 kHz (±20 Hz).[13] A Varian (Agilent) VNMRS (DirectDrive1) NMR spectrometer equipped with a 1.6 mm FastMAS probe operating at a ^{1}H frequency of 600 MHz was used. Ramped-amplitude cross-polarization magic-angle spinning (CPMAS) experiments were conducted with a cross-polarization time of 1−2 ms, a 10−20% linear ramp of the ^{1}H field strength during the CP time, and a 3-s recycle delay between successive acquisitions to identify the carbon-containing chemical groups based on their respective chemical shifts. ^{13}C Direct-polarization experiments (DPMAS) using a 100 s recycle delay were used to estimate the relative proportions of various carbon moieties via integration of specified spectral regions. The SPINAL method[24] was used to apply high-power heteronuclear ^{1}H decoupling of 170−185 kHz and low-power decoupling of 5 kHz in separate experiments. We repeated some measurements with ∼55 kHz SPINAL heteronuclear ^{1}H decoupling. Detailed experimental parameters for both CPMAS and DPMAS measurements have been described previously.[13,23,25]

The ^{13}C NMR data were typically processed with 100 or 200 Hz line broadening and analyzed independently using VNMRJ (version 3.1 Agilent Technologies, Santa Clara, CA) and ACD/NMR Processor Academic Edition (version 12; Advanced Chemistry Development, Inc., Toronto, ON, Canada, www.acdlabs.com, 2013). Chemical shifts were referenced externally to the methylene ($-CH_2-$) group of adamantane (Sigma-Aldrich) set to 38.48 ppm.

Integrated signal intensities were evaluated using both cut-and-weigh methods and counting of pixels using Photoshop software, designating the following chemical shift ranges for each major functional group: alkyl chains (8−50 ppm); alkoxy groups (50−92 ppm); arenes and alkenes (92−165 ppm); carboxyl and amide groups (165−185 ppm). Instrumental error limits (10−15%) were determined for the compositional analyses by repeating the DPMAS measurements using two different values of high-power ^{1}H decoupling. Biological error limits (∼15%) were evaluated from measurements on replicate RR cutin samples, as described previously.[13]

Assessments of molecular flexibility were made using several approaches.[8,26] (1) The fraction of "liquid-like" $(CH_2)_n$ groups, for which reorientation of the chain segments exceeds $\sim 10^5$ Hz, was measured for each cutin sample by comparing DPMAS NMR signal intensities with low-power (∼5 kHz) and high-power (∼175−180 kHz) ^{1}H decoupling. (2) The slow cooperative motions ($\sim 10^5$ s^{-1}, μs time scale) and rapid local motions ($\sim 10^8-10^9$ s^{-1}, ns time scale) were examined at each of several carbon sites of the cultivated (M82) and mutant cutins via solid-state NMR spin relaxation measurements. (3) Overall cooperative motions in a spatially defined region near the surface of interest were evaluated using stray field (unilateral) NMR to measure the spin echo decays for dewaxed M82 outer cuticles at the red-ripe (RR) developmental stage.

The relaxation measurements were carried out with 10 kHz (±20 Hz) MAS and a nominal set temperature of 25 °C. The recovery of ^{13}C signal intensity was observed following cross-polarization (CP) with a 2 ms contact time and inversion of the signal to determine the carbon spin−lattice relaxation times $T_1(C)$.[27] Values of $T_{1\rho}(H)$, the site-specific rotating-frame relaxation time for each ^{1}H nucleus directly bonded to an observed ^{13}C nucleus, were obtained with a Lee−Goldburg (LG) spin lock and LG cross-polarization period to suppress ^{1}H spin diffusion.[28,29] These latter experiments, which were conducted without rotor synchronization, used a short LGCP time (0.5 ms) and included 65−106 kHz LG pulses in separate experiments. Both $T_1(C)$ and $T_{1\rho}(H)$ relaxation data were fit using Origin software (OriginLab, Northampton, MA); the relaxation curve for each carbon resonance was obtained by fitting the maximal peak height to a single-exponential function.[30,31]

Unilateral NMR measurements were performed using an ACT MObile Universal Surface Explorer (NMR-MOUSE) (Magritek GmbH, Aachen, Germany) controlled by a Bruker Minispec spectrometer (Bruker BioSpin, Rheinstetten, Germany) operating at 18.5 MHz ^{1}H resonance frequency (0.5 T) with a field gradient G of 22.6 Tm^{-1} and a 90° pulse width of 4.5 μs. The instrument was equipped with a surface radio frequency (rf) coil creating a sensitive volume of about 10 × 10 mm^2 times an adjustable thickness of 2.5 mm away from the rf coil.[32] The transverse relaxation decays of ^{1}H nuclei were measured using the Carr−Purcell−Meiboom−Gill[33,34] pulse sequence with echo times of 30 μs and acquisition times of 100 μs that, in the presence of the field gradient G, defines a nominal resolution of about 100 μm. Thus, in contrast to the "bulk" properties assessed with the solid-state ^{13}C NMR measurements described above, the NMR-MOUSE probed molecular mobility in a spatial region near the cuticular surface.

Two biological replicates of the dewaxed red ripe tomato cuticle samples were examined using a recyle delay of 1 s, 1000 echoes, and 262144 scans at room temperature (∼25 °C). The tomato cuticles were compared to two commercial resin samples (poly(butylene terephthalate), and glycol-modified poly(ethylene terephthalate). These two samples are part of the ResinKit obtained from the Plastic Group of America (Woonsocket, RI, U.S.A.). The ResinKit provides samples and technical information on 50 of the most common industrially used thermoplastic resins (see Kehlet et al.[35] for further details).

RESULTS AND DISCUSSION

1. Dewaxed Inner and Outer Epidermal Cuticles Exhibit Divergent Chemical Compositions and Developmental Changes. Prompted by our description of a unique cuticle on the inner surface of tomato fruit pericarp tissues,[13] we sought insight into the structural differences between inner and outer epidermal layers that express 22 common genes involved in lipid metabolism but have contrasting functions as protective barriers in fluid flow and in tissue demarcation. Although both cuticle types constitute structural barriers that regulate the flow of water (between the locular cavity and the

DOI: 10.1021/acs.biomac.5b01321
Biomacromolecules 2016, 17, 215−224

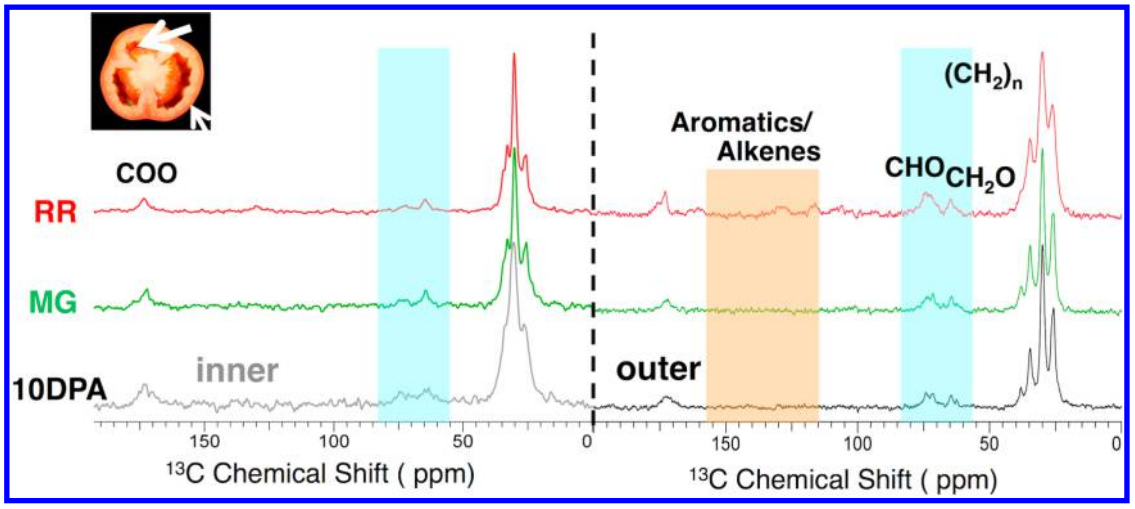

Figure 1. DPMAS ^{13}C NMR (150 MHz) of inner and outer epidermal wax-free cuticles (cutins, denoted pictorially) at 10 days postanthesis (DPA),[13] mature green (MG), and red ripe (RR) developmental stages. Highlighted spectral regions are described in the text.

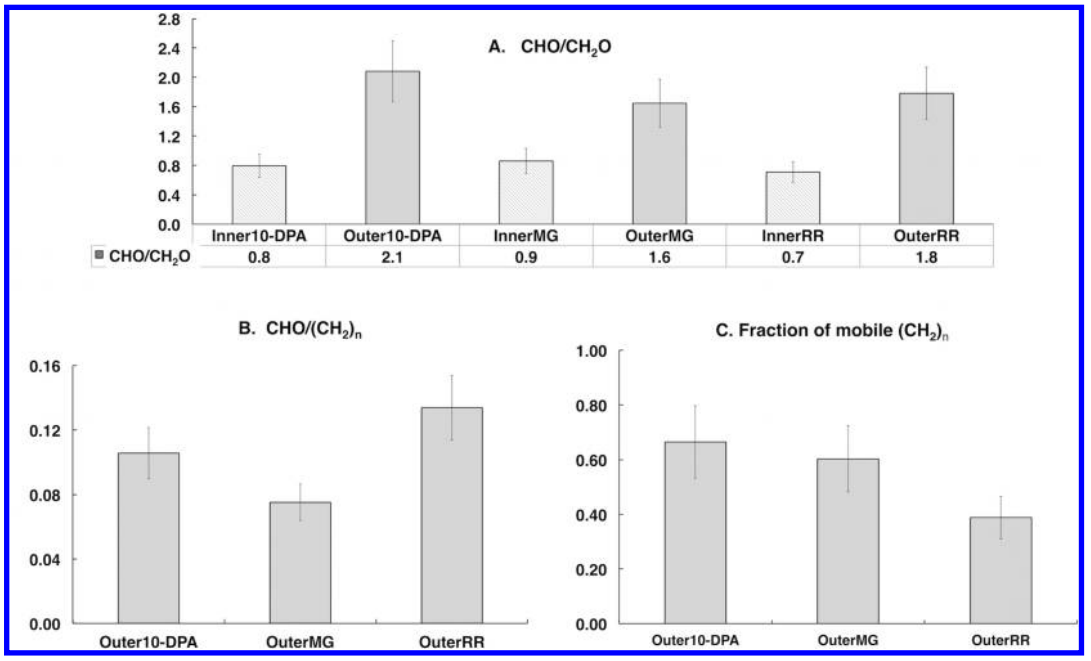

Figure 2. Ratios of carbon-containing functional groups and "liquid-like" acyl chain carbons[39] for M82 tomato fruit inner and outer epidermal (iep, oep) wax-free cuticles (cutins) derived from DPMAS ^{13}C NMR spectra obtained at an operating frequency of 150 MHz. (A) Ratios of CHO to CH_2O groups for iep vs oep cutins at each of 10 DPA, MG, and RR developmental stages. (B) Variation of CHO to $(CH_2)_n$ ratio for oep as a function of ripening stage. (C) Variation of "liquid-like" fraction of $(CH_2)_n$'s in oep cutins as a function of ripening stage.

pericarp and with the external environment, respectively), the inner cuticle (iep) has a distinctive role in preventing fusion of the placental tissues and the outer wall of the pericarp, whereas the outer cuticle (oep) uniquely maintains the structural integrity and microbial resistance of the fruit.[11] The inverted ratios of the predominant 16-hydroxypalmitic acid and 10,16-dihydroxypalmitic acid building blocks that are observed in iep and oep cutins at the 10 days postanthesis stage[13] suggest several working hypotheses. (a) Constituents capable of branching are disfavored in the inner epidermal cuticle, but close chain stacking and hydrogen bonding interactions are facilitated to form hydrophobically associated diffusion barriers. (b) Conversely, the branched constituents favored in outer cuticles have the potential to establish a network of cross-linked cutin macromolecular structures and midchain linkages to cell-wall polysaccharides (PS),[36] supporting proposed rationales for their mechanical strength.[37]

To assess differences in the developmental patterns of the plant biopolymer composites, we acquired solid-state ^{13}C NMR spectra to compare the molecular composition of intact inner and outer epidermal cutins at each of three ripening stages. Both cuticular polymers displayed carbon-containing functional groups that include long-chain aliphatics (20−40 ppm), oxygenated aliphatics (50−92 ppm), arenes and alkenes (92−165 ppm), and carboxyls (165−185 ppm; Figure 1). Within these structural classes, the oxygenated aliphatics can be designated separately as CH_3O (56 ppm), CH_2O (62 ppm), and CHO (72 ppm); long methylene chains ($(CH_2)_n$) display major peaks at 26, 29, and 33 ppm; esters and acids can contribute to the carboxyl resonances, but they share a

DOI: 10.1021/acs.biomac.5b01321
Biomacromolecules 2016, 17, 215−224

common chemical shift range. The amorphous character of these polymeric biomaterials produced a distribution of shifts for each chemical moiety and, thus, resulted in overlapping ^{13}C NMR resonances from structurally similar moieties. The chemical compositions estimated from peak areas of quantitatively reliable direct polarization magic-angle spinning (DPMAS) spectra (illustrated in Table S1) showed several distinctive trends that underscore their contrasting developmental progressions and physiological functions in the fruit.

We evaluated the balance of hydrophilic and hydrophobic carbon-containing moieties by measuring the ratio (COO + CHO + CH_2O + CH_3O)/$(CH_2)_n$. Both cutin polyesters and cuticularized polysaccharides[38] can contribute to the alkoxy ^{13}C NMR resonances. For instance, each of these constituents can contribute CHO signals derived from free CHOH or functionalized CHOC groups.[39] The ratio, which serves as a compositional indicator of the ability to interact with an aqueous or hydrophilic solvent, was found to be similar in magnitude (0.28 ± 0.02) for the inner and outer epidermal cutin materials. This result suggests a common hydrophilic−hydrophobic balance within the aliphatic biopolymer network that is consistent with their overlapping expression patterns of genes associated with cuticle metabolism[13] and their common functions as diffusion barriers that mediate interactions with water.[1,22] The compositional ratios conform to the structures of the principal C_{16}/C_{18} hydroxy fatty acid building blocks listed above[8,13,40,12] and should be altered only modestly if some midchain CHO groups are present. The ratios are also invariant with developmental stage, arguing against the formation of new aliphatic monomer structures during cuticle maturation and fruit ripening. Importantly, a clear dependence on epidermal cutin and developmental stage was found for relative peak intensities within the upfield ^{13}C NMR spectral envelope centered at ∼30 ppm, suggesting different degrees of midchain branching that would render the nearby long-chain methylene groups spectroscopically distinguishable.

To test for differences in cross-linking or branching capability for inner and outer epidermal cutins (dewaxed and enzymatically treated cuticles) at the three ripening stages, we first examined their CHO-to-CH_2O ratios (Figure 2A, shaded in blue). The oep cutin ratio is larger by 80−160%, depending on developmental stage. This relative preference for midchain CHOH groups and CHOC branches, as compared with linear polymer chains, is maintained for outer epidermal cutin across the three developmental stages. Moreover, this elevated proportion of cross-link-capable moieties within the outer epidermal supports previous biological findings in 10 DPA cutins from the M82 cultivar: (1) 40-fold higher CYP77A gene expression levels corresponding to a putative midchain hydroxylase enzyme; (2) the predominance of midchain-hydroxylated monomer units deduced from FT-IR of the polymeric cuticles and GC-MS of their soluble chemical breakdown products, respectively.[13]

A complementary assessment of cross-link capability as compared with acyl chain lengthening uses the ^{13}C NMR ratio of CHO to $(CH_2)_n$ groups present in long aliphatic chains (Figure 2B, Table S1). Whereas both cutin types exhibit ratios of ∼0.08 at 10 DPA and MG stages, the oep cutin value rises to 0.13 at the final RR stage. This trend is consistent with the following scenario: (1) commensurate increases in both chemical groups during fruit growth to the MG stage; (2) preferential formation of cross-linked or branched dendrimer-like structures[2] in the outer epidermal as the mature fruit turns red, whereby nearby cell-wall polysaccharides are "cutinized" and CHO spectral contributions are augmented; (3) ripening-associated formation of a dense interlaced surface cuticular network with a flatter long-range structure on the μm length scale.[41]

The thickening and increase in outer cutin-per-surface-area that have been observed progressively from 10 DPA to RR developmental stages[8,9,13] should be facilitated by a cross-linked structure that can foster interconnectivity of the polyesters or anchor them to waxes and polysaccharides.[19] This kind of macromolecular architecture should also support the deposition of hydrophobic aromatic moieties and pigments within the cutin polyester matrix.[3] Notably, preferential ripening-associated accumulation of phenolic compounds on the outer tomato fruit cuticle surface has been supported by ATR-FTIR measurements[42] and is now deduced by the appearance of multiply bonded and aromatic ^{13}C NMR resonances with respect to long-chain aliphatics (Figure 1, shaded in orange; Table S1). In turn, accumulation of phenolic compounds such as flavonoids during fruit ripening has been proposed to protect against UV radiation[43] and to impact cuticular mechanical properties by rigidifying the overall cutin biopolymer and/or particular cross-linked molecular segments.[1]

In addition to measuring the proportions of different carbon types, cross-link formation was evaluated from the fraction of comparatively flexible acyl chains ("liquid-like" flexibility in the parlance of solid-state NMR)[39] in these inner and outer epidermal cutins (Figure 2C), namely the fraction of DPMAS ^{13}C NMR signal intensity attributable to mobile $(CH_2)_n$'s (observed using low-power ^1H decoupling) compared with the total chain-methylene population (using high-power ^1H decoupling). As demonstrated previously for related plant cutin and suberin polymers,[26,44] these comparisons gauge the prevalence of microsecond molecular motions at those structural sites. The proportions for iep and oep cutins are similar (∼0.6) at the MG developmental stage, but drop to ∼0.4 for dewaxed RR outer epidermal tomato cutin, as expected if some branching occurs via midchain hydroxyl groups within supramolecular structures of the cutin polyester or with the associated cell-wall polysaccharides. This diminished "liquid-like" or flexible behavior of acyl chain segments is also understandable in light of the thickening and mechanical stiffening exhibited by outer tomato fruit cuticles upon ripening.[45] In summary, the cross-link-capable outer epidermal cutin structure retains considerable chain flexibility during fruit growth but becomes rigidified once expansion ceases and reddening occurs,[46] suggesting a design of the protective membrane assembly in which resilience is balanced against architectural strength.[1]

Finally, the increasing CHO/$(CH_2)_n$ ratio and decreasing "liquid-like", flexible fraction of $(CH_2)_n$ segments, both observed upon reddening for "bulk" outer epidermal cutin, prompted a complementary evaluation of overall molecular flexibility in a spatially defined region near the surface of interest. Stray field (unilateral) NMR was used to assess overall cooperative reorientation of ^1H nuclei[47,48] through their transverse relaxation and to compare the NMR signal decay for RR oep cutins with a panel of synthetic resins, including several engineered polyesters.[35] The dewaxed RR cutin samples displayed two-component spin echo decays with characteristic times of 0.15 ± 0.04 and 0.65 ± 0.4 ms; good agreement was observed between the two biological replicates. The relaxation decays in Figure 3 reveal that subsurface regions of the outer

DOI: 10.1021/acs.biomac.5b01321
Biomacromolecules 2016, 17, 215−224

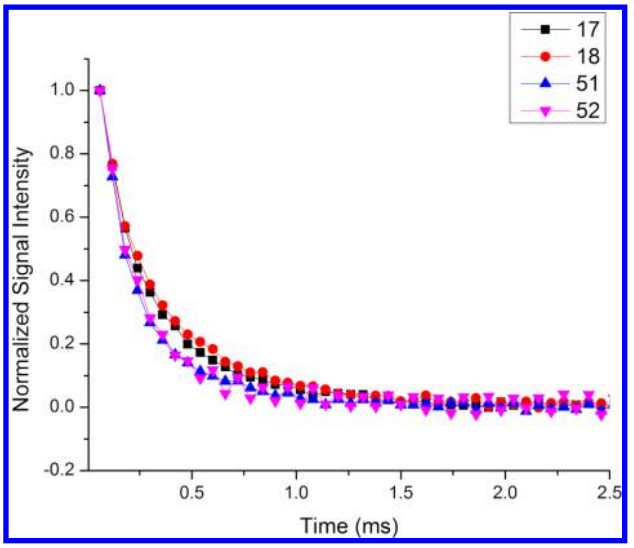

Figure 3. Transverse ^{1}H spin relaxation decays measured by unilateral NMR for dewaxed red ripe outer epidermal cuticles (cutins) from M82 tomato fruits and two synthetic resins,[35] showing consistency of two biological replicates (#51, #52) and discrimination with respect to the commercial polymers (shown by the different color coding). The polyesters poly(butylene terephthalate) (#17) and glycol-modified poly(ethylene terephthalate) (#18) are included for comparison.

RR tomato cutins (#51, #52) are fairly rigid with respect to the 50 commercial resins in the ResinKit,[35] reproducibly displaying similar flexibility to the poly(butylene terephthalate) and glycol-modified poly(ethylene terephthalate) thermoplastic polyesters in the group (#17, #18). These surface-specific cuticular rigidity trends also conform with indications of cross-linking or branching propensity and attenuated "liquid-like" chain segment reorientation deduced from DPMAS ^{13}C NMR signal intensities of the "bulk" RR outer epidermal cutins.

Taken together, the ^{13}C NMR spectral results suggest that maturation of the tomato outer epidermal cutin retains the hydrophilic−hydrophobic balance of the aliphatic framework while building rigidified branched structures once the fruit has attained its maximum size. In addition to ensuring compatibility of both inner and outer epidermal cuticular tissues with the underlying PS cell walls, the amphipathic hydroxy fatty acid structures support the function of the outer epidermal cuticles in particular, facilitating the buildup of hydrophobic pigments that can interact favorably with waxes to form a thicker protective seal that resists desiccation and microbial invasion, and that can provide greater mechanical strength.[26,42,49,50]

2. Single-Gene Mutations Alter Molecular Flexibilities in Red Ripe Outer Epidermal Cutins. The significant loss of acyl chain segmental mobility observed for the outer epidermal cutins at the red ripe developmental stage led us to undertake an in-depth ^{13}C CPMAS NMR dynamic study of the "solid-like"(cross polarizable) carbon moieties in a series of tomato lines with single-gene mutations and altered fruit cuticle phenotypes. To probe both local motions occurring at resonance frequencies of ~10^{8}−10^{9} s^{-1} and cooperative

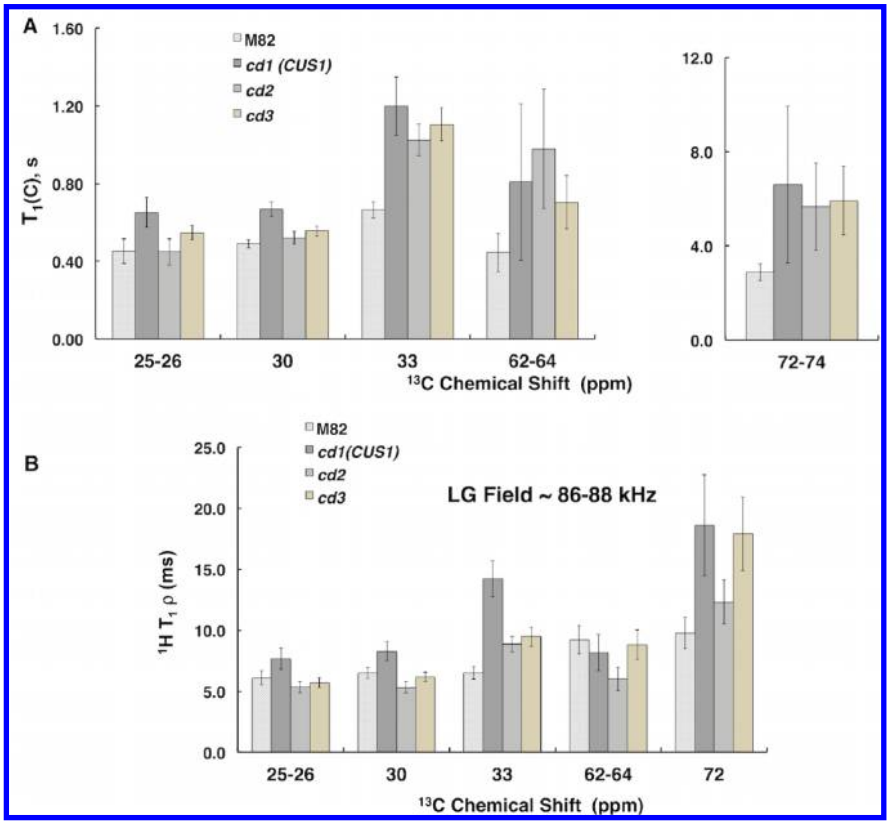

Figure 4. ^{13}C spin relaxation times measured at 150 MHz for outer epidermal (oep) tomato cutins from red ripe fruit of a control cultivar (M82) and its single-gene mutants (*cd1*, *cd2*, *cd3*). (A) Spin−lattice relaxation times, T_1(C), for molecular moieties including long-chain methylenes (25, 30, and 33 ppm), oxymethylenes (63 ppm), and oxymethines (73 ppm). (B) Rotating-frame spin relaxation times, $T_{1\rho}$(H), measured with a Lee−Goldburg (LG) spin-lock field of ~87 kHz via the respective attached carbons with chemical shifts noted above. Additional measurements with a LG field of 90−106 kHz appear in Figure S1.

DOI: 10.1021/acs.biomac.5b01321
Biomacromolecules 2016, 17, 215−224

motions occurring at rates of ~10^5 s^{-1} at particular molecular sites, a series of NMR relaxation experiments was conducted on fruits with glossy surfaces.[8] As demonstrated previously for fruit cuticles[44,51] and both control and genetically modified potato periderms,[26,52] site-specific assessments of cuticular flexibility on both microsecond (μs) and nanosecond (ns) time scales offer insights into the resiliency and cracking resistance of these plant polymeric materials.

Figure 4A illustrates the values of T_1(C) that reflect local segmental motions occurring on the ns time scale for particular carbon-containing functional groups and tomato lines. For both synthetic polyesters[53,54] and biopolymer assemblies, including fruit cuticles,[22,39,55] polymer performance benchmarks such as the bulk modulus depend upon this mode of molecular reorientation and can be modulated by either humidity or temperature.[44,56] In these fruit cutins, related cuticles, and potato tuber periderms,[26,44,51] rapid motions are most efficient for the acyl chains (25 and 30 ppm) and least efficient for the CHO groups of cross-link-capable esters/alcohols and attached cell-wall polysaccharide components (72 ppm). Thus, the site-specific T_1(C) trends reflect local motional restrictions at potential linkage sites between the hydroxyfatty acid chains and polysaccharide cell walls. This contrasting dynamic behavior is observed consistently, although the numerical comparisons with related samples are approximate because of differences in NMR magnetic field strength, wax load, and fractions of cross-polarizable (relatively rigid) carbons that are being observed in the spin relaxation experiments. Because the *cd(n)* materials have tripled proportions of "liquid-like" $(CH_2)_n$ groups,[8] we might expect (but did not observe) their remaining solid-like chain segments to reorient less efficiently and yield longer T_1(C) values compared with the M82 cutin.[44,51] Notably, the acyl chain carbon segments resonating at 33 ppm are rigid enough to be considered semicrystalline; that trend can be attributed to proximity to polysaccharide anchoring sites[26,52,57] in potato periderms and, by analogy, to those tomato fruit cuticle layers that are embedded with cell-wall PS.[1,38]

Each of the three single-gene mutants, which have significantly reduced outer epidermal fruit cutin content and consequent anomalies in architecture, surface stiffness, and susceptibility to microbial infection,[8] displayed ~2-fold less efficient ns motions of their CHO and CH_2O groups with respect to the M82 cultivar, but the spin−lattice relaxation times (T_1(C)) of these functional groups were similar in magnitude for the *cd1*, *cd2*, and *cd3* fruits. Comparing these two types of alkoxy groups, local motions of the CHO carbons are less efficient by factors of 6−8 than CH_2O groups for M82 and its mutants, underscoring the rigidity of cross-link-capable segments that include the CHO carbons. Again, the site-specific T_1(C) trends reflect local motional restrictions at potential linkage sites between the hydroxy fatty acid chains and polysaccharide cell walls. An analogous variation was reported in suberized potato tuber periderms, for which ns motions (local motions) are severely attenuated because CHO groups are linked to the cell-wall polysaccharides.[26] To account for the relative inefficiency of local CH_nO reorientation of the mutant outer epidermal cutins in terms of gene-mediated changes in macromolecular architecture, we note a doubling of the compositional ratio (CHO + CH_2O + CH_3O + COO)/($(CH_2)_n$ + aromatics)[8] (Figure 5B), which could facilitate hydrogen-bonding and cross-linking with polysaccharides in the cuticularized layer.[1,38] This rationale for the attenuation of segmental reorientation for CH_nO groups of the *cd(n)* outer

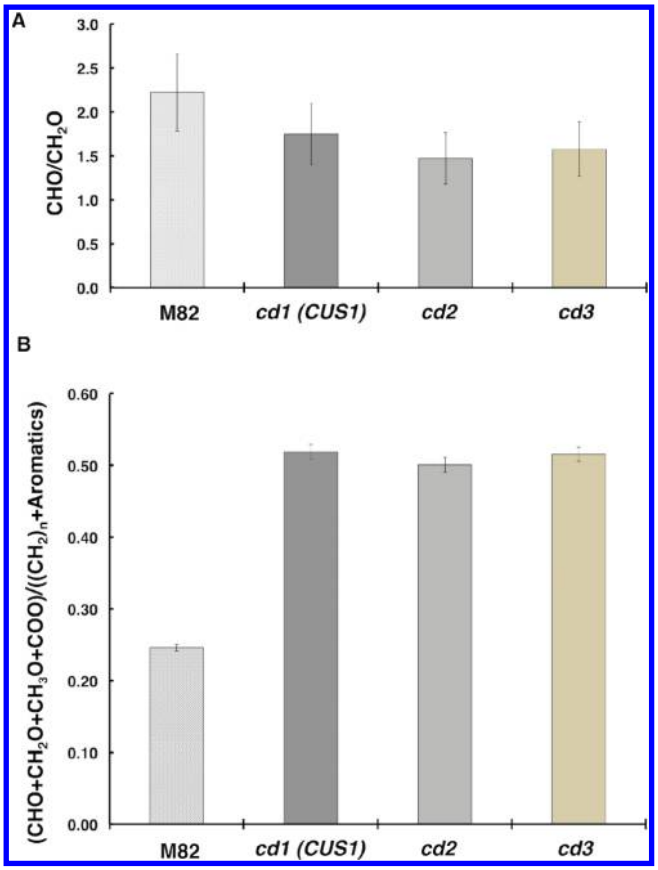

Figure 5. Ratios of carbon-containing functional groups for outer epidermal tomato cutins from control (M82) and single-gene mutant *(cd1 (CUS1), cd2, cd3)* red ripe cultivars, derived from DPMAS ^{13}C NMR spectra obtained at an operating frequency of 150 MHz with ^1H decoupling power corresponding to 175−180 kHz (Figure S2). (A) Ratios of CHO to CH_2O groups. (B) Ratios of (CHO + CH_2O + CH_3O + COO) to [$(CH_2)_n$ + aromatics] chemical groupings.

epidermal cutins is also supported by trends in cuticular content and ultrastructure: only modest amounts of ester-derived monomers are obtained from their chemical depolymerization, their anomalously thin cuticles are more likely to have connections to the rigid PS cell walls, and their ^{13}C NMR spectra have elevated contributions from PS-derived CH_nO moieties.[8]

Complementary information on site-specific cooperative motions that occur on the microsecond time scale was deduced from the Lee−Goldburg spin-lock rotating-frame spin relaxation times ($T_{1\rho}$(H)) summarized in Figure 4B. These slower overall dynamic processes have been linked to the impact strength or toughness of glassy synthetic polycarbonates.[58] With the rotating-frame relaxation limited to particular chemical sites rather than potentially averaged by spin diffusion, we observed a slower relaxation process than in the corresponding traditional $\langle T_{1\rho}(H)\rangle$ experiment.[44] Among the long-chain methylene groups appearing at 25−35 ppm in the ^{13}C NMR spectrum, the resonance at 33 ppm displays markedly less efficient cooperative motions for the three mutants, especially for *cd1*. The overall trend parallels the local segmental rigidity deduced from T_1(C) data as reported in other plant cell-wall systems[29] and again suggests anchoring of these methylenes by nearby cell-wall polysaccharides.[26,52,57] This explanation is supported by the concurrent observation of

DOI: 10.1021/acs.biomac.5b01321
Biomacromolecules 2016, 17, 215−224

diminished microsecond segmental motions, by nearly 2-fold for *cd1* and *cd3* among the single-gene mutant oep cutins, when observed for the 72-ppm CHO resonance attributable to cell-wall polysaccharides and midchain cutin branches. This overall dearth of μs motions (cooperative motions) in cross-link-capable and polysaccharide-associated regions of the mutant tomato cutins is also revealed by comparing the $T_{1\rho}$(H)s for CHO (72 ppm) versus CH_2O (63 ppm) groups: those values are comparable at the oxymethine and oxymethylene sites for M82 cutins but doubled for CHO groups of *cd1*, *cd2*, and *cd3* (*cd(n)*) mutants. As noted above, the abundant proximal cutin−polysaccharide interactions present in the outer cuticle layers[1,59] of the mutant fruits offer an architectural rationale for the relative lack of cooperative motions, evidenced for both methylene chain carbons at 33 ppm and oxymethines (CHO) at 72 ppm.

The overall similarity of both T_1(C) and $T_{1\rho}$(H) spin relaxation times for outer epidermal fruit cutin from *cd1*, *cd2*, and *cd3* mutants conforms with the respective chemical compositions displayed in Figure 5. Specifically, their measures of hydrophilic−hydrophobic balance [$(CHO/(CH_2)_n$ reported previously[8] and $(CHO + CH_2O + CH_3O + COO)/[(CH_2)_n$ + aromatics], measured herein] are similarly elevated, facilitating polyester−polysaccharide linkages[36] that attenuate local and cooperative molecular flexibility. The CHO/CH_2O ratios are also modestly but comparably diminished for all mutants with respect to the M82 control cultivar. Finally, the more prominent CH_3O resonances displayed in ^{13}C NMR spectra of the mutants (Figure S2) can be attributed to cutinized polysaccharides that are retained after enzymatic treatment with cellulase and pectinase. Taken together, the relaxation and compositional trends support changes in macromolecular architecture that can promote cutin−polysaccharide interactions in the relatively hydrophilic cuticularized layer. However, the diminished relative numbers of aliphatic chain carbons and absolute amounts of cutin could result in sparse cutin−wax interactions in the cuticle proper,[1,59] resulting in the formation of comparatively stiff wax-rich cuticular surfaces.[8]

3. Tomato Cutins Offer Design Guidelines for Assembling a Robust Biopolymer Composite. Functional attributes such as waterproofing and viscoelasticity pertain, respectively, to the surface and mechanical behavior of the cuticle, but their underlying origins are tied inextricably to molecular composition and flexibility. Thus, we sought to delineate the compositional and motional criteria that govern the architecture of these versatile plant cuticular biopolymer assemblies.

The current comparisons of plant cutins, whether between inner and outer epidermal or among outer cuticles in control cultivars versus single-gene mutants, illustrate how a single set of primarily (hydroxy)fatty acid building blocks can meet the design requirements of diverse plant functions. Thus, an optimally functioning outer epidermal layer should exhibit a hydrophilic−hydrophobic balance of cutin polyesters and cutin-linked cell-wall polysaccharides that promotes both hydrophobic interactions with adjoining waxes (of the cuticle proper) and attachment of cutin to polysaccharides (of the cuticularized layer).[38] Meeting those architectural requirements can facilitate the thickening of the cuticle that occurs during maturation and ripening, because additional layers will have energetically favorable interactions with either wax or polysaccharide constituents. In addition to thickening, cuticular mechanical integrity can be achieved if the cutin possesses substantial cross-link-capable CHO groups that facilitate deposition of phenolic compounds.[42] Finally, the regulation of water permeability via hydrophilic interactions and hydrophobic repellency[22] requires a molecular architecture that incorporates both of these contrasting characteristics. In polyester−polysaccharide−wax composites, architectural designs that favor chemical interactions required for protective function can thus be achieved by maintaining appropriate values of the functional group ratios $(COO + CHO + CH_2O + CH_3O)/[(CH_2)_n$ + aromatics] and $CHO/(CH_2)_n$ (Figure 2B).

However, contrasting molecular architectures are favored compositionally for cuticles of the inner epidermal and for outer epidermal of the *cd1*, *cd2*, and *cd3* single-gene mutants (considered together as *cd(n)*). Both types of tomato cutins exhibit anomalous values of the $CHO/(CH_2)_n$[10] and CHO/CH_2O ratios at the red ripe developmental stage (Figures 2A and 5A). For M82 inner epidermal cuticles, the small proportions of CHO groups can be linked to diminished midchain hydroxylation, a design that makes sense functionally to promote close chain packing when connections to polysaccharides are not required to thicken or strengthen the barrier. For outer cuticles of the *cd(n)* mutants, it is less reliable to interpret these compositional ratios in terms of cross-linking capabilities for the cutin polymers: their dramatically reduced amounts imply that this NMR-based compositional ratio could also include substantial contributions from cutinized polysaccharides. Despite a dearth of polyesters available to associate with the cell-wall polysaccharides, however, waterproofing function is maintained by the outer epidermal cuticles of these mutant fruits through an alternative biosynthetic redesign that is rich in waxes.[8]

The correlations observed between cuticular chemical composition and barrier function can be more deeply understood by consideration of the molecular flexibility, resiliency, and transport properties of the resulting plant membranes. Indeed, the role of molecular dynamics as a link between polymer structure and function is well established for both synthetic and biological macromolecules.[44,60] This principle is illustrated first by our findings for tomato fruit ripening, which reveal diminishing proportions of "liquid-like" acyl chain segments[39,44] as the outer cuticle is strengthened by changes that include cross-linking to cell-wall polysaccharides, layer thickening, and deposition of phenolic moieties.[26,42,50] By this measure, RR cutins from the oep are comparably flexible to native enzymatically treated and dewaxed potato periderms,[26] but considerably more rigid than waxy tomato cuticles.[44] Their subsurface spatial regions have transverse relaxation properties that suggest a substantial degree of overall molecular rigidity, similar to the polyesters among a panel of 50 industrial resins.

Second, the balanced hydrophilic−hydrophobic molecular profiles measured herein permit versatile interactions of the fruit cuticles with water and waxes, each of which alters their local or overall flexibility. Hydration via CHO or C═O groups[42] plasticizes the membrane, enhancing both μs motions at cross-link sites and ns motions of remote hydrophobic $(CH_2)_n$ segments of the biopolyester network,[22,61] hence suggesting the facilitation of permeability and avoidance of membrane cracking for these glassy biopolymers.[62] Such plasticizing effects and correlations with mechanical toughness are well documented in, for example, epoxy resins[63] and glassy polycarbonates,[58] and so the cutin polymer potentially extends this trend to include biopolyesters. By contrast, hydration produces the opposite trend in overall μs motions for native

DOI: 10.1021/acs.biomac.5b01321
Biomacromolecules 2016, 17, 215−224

waxy tomato cuticles.[44] The alteration of outer epidermal cuticle flexibility and resiliency by waxes per se is exemplified by the wax-rich *cd(n)* mutants, which display high surface moduli and poor microbial defense capabilities that have been proposed to reflect the greater crystallinity, surface roughness, and cracking propensity of their stiffer cuticular membranes.[8]

We note that the *cd(n)* cutin motional profile is unlikely to be the sole contributor to the properties of the corresponding outer fruit cuticles, which contain normal amounts of wax but only 2−5% of the polyesters present in control cultivars. For instance, the solid-like population of ^{13}C nuclei in *cd(n)* cutins displays attenuated motions of both the 33-ppm $(CH_2)_n$ groups and the abundant 72-ppm CHO carbons; these trends include both local and cooperative motions that occur on the nanosecond and microsecond time scales, respectively. Although we observed elevated hydrophilic−hydrophobic ratios and associated cross-link capabilities that could rationalize these trends, the diminished amount of cutin present in these mutants can itself account for an outer epidermal membrane dominated by stiff waxy layers[8] and will provide very few of the high-specific-heat constituents needed for efficient thermostatic function.[64]

The study of cutin-deficient mutants also offers an excellent opportunity to link cutin biosynthesis with the functional characteristics of protective cuticular membranes.[8,65] First, diminished cutin content within the waxy cuticle proper could reduce the overall specific heat and compromise thermoregulatory capabilities as described above.[64] Analogously, modest cutin content with respect to polysaccharide components in the cuticularized layer maintains the inefficiency of collective motions at CHO (vs CH_2O) molecular sites, weakening the resiliency that could prevent cracking of cultivated fruits. Nonetheless, both types of alkoxy groups can interact favorably with water, plasticizing the cuticle[22,44] and allowing for water permeation through a largely lipophilic covering that lacks pores. The latter type of physicochemical analysis has been conducted, for instance, to evaluate cured bisphenol A diglycidyl ether epoxy resins and copolyester thermoplastic elastomers used in adhesives and automotive parts, respectively.[54,63] And importantly, the potential usefulness of such biologically inspired molecular design trends is illustrated by a host of emerging products derived from renewable cuticular polyester sources: oil−water surfactant emulsions with cosmetic or pharmacological applications,[66] cross-linked polyester fibers for packaging products,[6,67] and suberin-based films with waterproofing and bactericidal capabilities,[68] to name just a few applications.

CONCLUSIONS

Protective plant materials such as cutin are multifunctional polymeric composites that have evolved to ensure mechanical integrity, regulate water and heat transport, and protect against damage from both radiation and microbes. In addition, plant cuticles offer a naturally occurring source of surfactants used in cosmetics, packaging materials, coatings, and pharmaceuticals. Using tomato fruit lines with contrasting protective cuticular layers and developmental stages as model systems, solid-state NMR measurements have enabled us to identify elements of chemical composition and molecular dynamics that are essential to the macromolecular architecture of cutin polyesters associated with cell-wall polysaccharides and hydrophobic waxes. The hydrophilic−hydrophobic balance of the tomato outer epidermal cutin promotes the formation of cutinized cell walls analogously to recently characterized suberized potato periderms,[26] and both biomaterials also exhibit networked architectures that are suitable for deposition of aromatic and waxy waterproofing compounds. Notable structural changes of the outer epidermal cutins during fruit ripening, which include enhanced proportions of cross-link-capable oxygenated aliphatic groups and diminished fractions of comparatively flexible "liquid-like" acyl chain segments, conform to their developmentally signaled roles in mechanical strengthening via cross-links and noncovalent association. Several cutin-deficient tomato mutants with stiffened surfaces and compromised resistance to microbial infection[8] are found to have less efficient local and cooperative motions, demonstrating the importance of combining mechanical strength with resiliency to establish a robust protective membrane that can resist fracture and microbial invasion.

ASSOCIATED CONTENT

Supporting Information

The Supporting Information is available free of charge on the ACS Publications website at DOI: 10.1021/acs.biomac.5b01321.

Rotating-frame spin relaxation times, $T_{1\rho}(H)$, measured with a Lee−Goldburg (LG) spin-lock field of ∼90−106 kHz via the respective attached carbons; 150 MHz DPMAS ^{13}C NMR spectra obtained at 10 kHz MAS, with ^{1}H decoupling power corresponding to 175−180 kHz (PDF).

AUTHOR INFORMATION

Corresponding Author

*E-mail: rstark@ccny.cuny.edu.

Present Addresses

[§]Instituto de Hortofruticultura Subtropical y Mediterránea "La Mayora", Universidad de Málaga, Consejo Superior de Investigaciones Científicas, Facultad de Ciencias, Campus de Teatinos s/n, 29071 Málaga, Spain.

[∥]Department of Fruit Tree Sciences, Newe Ya'ar Research Center, Agricultural Research Organization, P.O. Box 1021, Ramat Yishay 30095, Israel.

Notes

The authors declare no competing financial interest.

ACKNOWLEDGMENTS

The authors would like to acknowledge Dr. Hsin Wang for his valuable technical assistance with the NMR instrument. Financial support for this work is gratefully acknowledged from the U.S. National Science Foundation (NSF MCB-0843627, 1411984, and 0741914 to R.E.S.), the U.S. National Science Foundation Plant Genome Research Program (IOS-1339287 to J.K.C.R.), and the Agriculture and Food Research Initiative Competitive Grants Program of the U.S.D.A. National Institute of Food and Agriculture (2011−67013−19399 to J.K.C.R.). A.J.M. was supported by a postdoctoral award MEC/Fulbright by the Spanish Ministerio de Educación y Ciencia (FU2005−0883). T.I. was supported by a Postdoctoral Award FI-375-2005 from the United States−Israel Binational Agricultural Research and Development Fund. NMR resources were supported by The City College of New York (CCNY) and the CUNY Institute of Macromolecular Assemblies, with infrastructural assistance provided by the National Institute on

DOI: 10.1021/acs.biomac.5b01321
Biomacromolecules 2016, 17, 215−224

Minority Health and Health Disparities (8G12 MD007603−29).

REFERENCES

(1) Bargel, H.; Koch, K.; Cerman, Z.; Neinhuis, C. *Funct. Plant Biol.* **2006**, *33*, 893.
(2) Pollard, M.; Beisson, F.; Li, Y.; Ohlrogge, J. B. *Trends Plant Sci.* **2008**, *13*, 236−246.
(3) Beisson, F.; Ohlrogge, J. *Nat. Chem. Biol.* **2012**, *8*, 603−604.
(4) Bernards, M. A. *Can. J. Bot.* **2002**, *80*, 227−240.
(5) Ranathunge, K.; Schreiber, L.; Franke, R. *Plant Sci.* **2011**, *180*, 399−413.
(6) Vilela, C.; Sousa, A. F.; Fonseca, A. C.; Serra, A. C.; Coelho, J. F. J.; Freirea, C. S. R.; Silvestre, A. J. D. *Polym. Chem.* **2014**, *5*, 3119−3141.
(7) Gandini, A.; Lacerda, T. M. *Prog. Polym. Sci.* **2015**, *48*, 1.
(8) Isaacson, T.; Kosma, D. K.; Matas, A. J.; Buda, G. J.; He, Y.; Yu, B.; Pravitasari, A.; Batteas, J. D.; Stark, R. E.; Jenks, M. A.; Rose, J. K. C. *Plant J.* **2009**, *60*, 363−377.
(9) Girard, A.-L.; Mounet, F.; Lemaire-Chamley, M.; Gaillard, C.; Elmorjani, K.; Vivancos, J.; Runavot, J.-L.; Quemener, B.; Petit, J.; Germain, V.; Rothan, C.; Marion, D.; Bakan, B. *Plant Cell* **2012**, *24*, 3119−3134.
(10) Serra, O.; Chatterjee, S.; Huang, W.; Stark, R. E. *Plant Sci.* **2012**, *195*, 120−124.
(11) Seymour, G. B.; Ostergaard, L.; Chapman, N.; Knapp, S.; Martin, C. *Annu. Rev. Plant Biol.* **2013**, *64*, 219−241.
(12) Yeats, T. H.; Rose, J. K. C. *Plant Physiol.* **2013**, *163*, 5−20.
(13) Matas, A. J.; Yeats, T. H.; Buda, G. J.; Zheng, Y.; Chatterjee, S.; Tohge, T.; Ponnala, L.; Adato, A.; Aharoni, A.; Stark, R. E.; Fernie, A. R.; Fei, Z.; Giovannoni, J. J.; Rose, J. K. C. *Plant Cell* **2011**, *23*, 3893−3910.
(14) Yeats, T. H.; Martin, L. B. B.; Viart, H. M.-F.; Isaacson, T.; He, Y.; Zhao, L.; Matas, A. J.; Buda, G. J.; Domozych, D. S.; Clausen, M. H.; Rose, J. K. C. *Nat. Chem. Biol.* **2012**, *8*, 609−611.
(15) Yeats, T. H.; Huang, W.; Chatterjee, S.; Viart, H. M. F.; Clausen, M. H.; Stark, R. E.; Rose, J. K. C. *Plant J.* **2014**, *77*, 667−675.
(16) Heredia-Guerrero, J. A.; Benitez, J. J.; Heredia, A. *BioEssays* **2008**, *30*, 273−277.
(17) Dominguez, E.; Heredia-Guerrero, J. A.; Benitez, J. J.; Heredia, A. *Mol. BioSyst.* **2010**, *6*, 948−950.
(18) Domínguez, E.; Fernández, M. D.; Hernández, J. C. L.; Parra, J. P.; España, L.; Heredia, A.; Cuartero, J. *Physiol. Plant.* **2012**, *146*, 473−486.
(19) Domínguez, E.; Heredia-Guerrero, J. A.; Heredia, A. *New Phytol.* **2011**, *189*, 938−949.
(20) Shi, J. X.; Adato, A.; Alkan, N.; He, Y.; Lashbrooke, J.; Matas, A. J.; Meir, S.; Malitsky, S.; Isaacson, T.; Prusky, D.; Leshkowitz, D.; Schreiber, L.; Granell, A. R.; Widemann, E.; Grausem, B.; Pinot, F.; Rose, J. K. C.; Rogachev, I.; Rothan, C.; Aharoni, A. *New Phytol.* **2013**, *197*, 468−480.
(21) Schonherr, J.; Riederer, M. *Plant, Cell Environ.* **1986**, *9*, 459−466.
(22) Round, A. N.; Yan, B.; Dang, S.; Estephan, R.; Stark, R. E.; Batteas, J. D. *Biophys. J.* **2000**, *79*, 2761−2767.
(23) Chatterjee, S.; Sarkar, S.; Oktawiec, J.; Mao, Z.; Niitsoo, O.; Stark, R. E. *J. Visualized Exp.* **2012**, 1−7 and e529.
(24) Fung, B. M.; Khitrin, A. K.; Ermolaev, K. *J. Magn. Reson.* **2000**, *142*, 97−101.
(25) Chatterjee, S.; Santos, F.; Abiven, S.; Itin, B.; Stark, R. E.; Bird, J. A. *Org. Geochem.* **2012**, *51*, 35−44.
(26) Serra, O.; Chatterjee, S.; Figueras, M.; Molinas, M.; Stark, R. E. *Biomacromolecules* **2014**, *15*, 799−811.
(27) Torchia, D. A. *J. Magn. Reson.* **1978**, *30*, 613−616.
(28) Huster, D.; Xiao, L.; Hong, M. *Biochemistry* **2001**, *40*, 7662−7674.
(29) Dick-Pérez, M.; Zhang, Y.; Hayes, J.; Salazar, A.; Zabotina, O. A.; Hong, M. *Biochemistry* **2011**, *50*, 989−1000.
(30) Hediger, S.; Emsley, L.; Fischer, M. *Carbohydr. Res.* **1999**, *322*, 102−112.
(31) Masuda, K.; Tabata, S.; Sakata, Y.; Hayase, T.; Yonemochi, E.; Terada, K. *Pharm. Res.* **2005**, *22*, 797−805.
(32) Perlo, J.; Casanova, F.; Blümich, B. *J. Magn. Reson.* **2005**, *176*, 64−70.
(33) Carr, H.; Purcell, E. *Phys. Rev.* **1954**, *94*, 630−638.
(34) Meiboom, S.; Gill, D. *Rev. Sci. Instrum.* **1958**, *29*, 688−691.
(35) Kehlet, C.; Del Federico, E.; Schahbaz, H.; Catalano, A.; Dittmer, J.; Nielsen, N. C. *Anal. Methods* **2013**, *5*, 4480−4486.
(36) Tian, S.; Fang, X.; Wang, W.; Yu, B.; Cheng, X.; Qiu, F.; Mort, A. J.; Stark, R. E. *J. Agric. Food Chem.* **2008**, *56*, 10318−10325.
(37) Bargel, H.; Neinhuis, C. *J. Exp. Bot.* **2005**, *56*, 1049−1060.
(38) Jeffree, C. E. In *Biology of the Plant Cuticle*; Riederer, M., Muller, C., Eds.; Wiley, 2006; pp 11−125.
(39) Zlotnik-Mazori, T.; Stark, R. E. *Macromolecules* **1988**, *21*, 2412−2417.
(40) Kosma, D. K.; Parsons, E. P.; Isaacson, T.; Lü, S.; Rose, J. K. C.; Jenks, M. A. *Physiol. Plant.* **2010**, *139*, 107−117.
(41) Benitez, J. J.; Matas, A. J.; Heredia, A. *J. Struct. Biol.* **2004**, *147*, 179−184.
(42) Heredia-Guerrero, J. A.; Benitez, J. J.; Dominguez, E.; Bayer, I. S.; Cingolani, R.; Athanassiou, A.; Heredia, A. *Front. Plant Sci.* **2014**, *5*, 1−14.
(43) Kolb, C. A.; Pfündel, E. E. *Plant, Cell Environ.* **2005**, *28*, 580−590.
(44) Stark, R. E.; Yan, B.; Stanley-Fernandez, S. M.; Chen, Z.-J.; Garbow, J. R. *Phytochemistry* **2008**, *69*, 2689−2695.
(45) España, L.; Heredia-Guerrero, J. A.; Segado, P.; Benítez, J. J.; Heredia, A.; Domínguez, E. *New Phytol.* **2014**, *202*, 790−802.
(46) Bargel, H.; Neinhuis, C. *J. Plant Growth Regul.* **2004**, *23*, 61−75.
(47) Blümich, B.; Perlo, J.; Casanova, F. *Prog. Nucl. Magn. Reson. Spectrosc.* **2008**, *52*, 197−269.
(48) Blümich, B.; Casanova, F.; Perlo, J.; Presciutti, F.; Anselmi, C.; Doherty, B. *Acc. Chem. Res.* **2010**, *43*, 761−770.
(49) Kerstiens, G. *Trends Plant Sci.* **1996**, *1*, 125−129.
(50) Borisjuk, N.; Hrmova, M.; Lopato, S. *Biotechnol. Adv.* **2014**, *32*, 526−540.
(51) Garbow, J. R.; Stark, R. E. *Macromolecules* **1990**, *23*, 2814−2819.
(52) Stark, R. E.; Garbow, J. R. *Macromolecules* **1992**, *25*, 149−154.
(53) Schaefer, J.; Stejskal, E. O.; Buchdahl, R. *Macromolecules* **1975**, *8*, 291−296.
(54) Jelinski, L. W.; Schilling, F. C.; Bovey, F. A. *Macromolecules* **1981**, *14*, 581−586.
(55) Batteas, J. D.; Stark, R. E. In *Molecular Interfacial Phenomena of Polymers and Biopolymers*; Chen, P., Ed.; Abington Hall, Woodhead Publishing Co.: Cambridge, U.K., 2005; pp 580−608.
(56) Matas, A. J.; Lopez-Casado, G.; Cuartero, J.; Heredia, A. *Am. J. Bot.* **2005**, *92*, 462−468.
(57) Gil, A. M.; Lopes, M.; Rocha, J.; Neto, C. P. *Int. J. Biol. Macromol.* **1997**, *20*, 293−305.
(58) Schaefer, J.; Stejskal, E. O.; Buchdahl, R. *Macromolecules* **1977**, *10*, 384−405.
(59) Jeffree, C. E. *Plant Cuticles and Integrated Functional Approach*; Bios Scientific Publishers, Ltd.: Oxford, U.K., 1996; Vol. Kerstiens, pp 33−82.
(60) North, A. M. *Molecular Behavior and the Development of Polymeric Materials*; Ledwith, A., North, A. M., Eds.; Wiley: New York, 1975.
(61) Petracek, P. D.; Bukovac, M. J. *Plant Physiol.* **1995**, *109*, 675−679.
(62) Luque, P.; Heredia, A. *Plant Physiol. Biochem.* **1997**, *35*, 251−256.
(63) Jelinski, L. W.; Dumais, J. J.; Cholli, A. L.; Ellis, T. S.; Karasz, F. E. *Macromolecules* **1985**, *18*, 1091−1095.
(64) Heredia, A. *Biochim. Biophys. Acta, Gen. Subj.* **2003**, *1620*, 1−7.
(65) Domínguez, E.; Heredia-Guerrero, J. A.; Heredia, A. *Trends Plant Sci.* **2015**, *20*, 1−8.

DOI: 10.1021/acs.biomac.5b01321
Biomacromolecules 2016, 17, 215−224

(66) Fameau, A.-L.; Gaillard, C.; Marion, D.; Bakan, B. *Green Chem.* **2013**, *15*, 341−346.
(67) Benítez, J. J.; Heredia-Guerrero, J. A.; Guzmán-Puyol, S.; Domínguez, E.; Heredia, A. *J. Appl. Polym. Sci.* **2015**, *132*, 1−7.
(68) Garcia, H.; Ferreira, R.; Martins, C.; Sousa, A. F.; Freire, C. S. R.; Silvestre, A. J. D.; Kunz, W.; Rebelo, L. P. N.; Silva Pereira, C. *Biomacromolecules* **2014**, *15*, 1806−1813.

DOI: 10.1021/acs.biomac.5b01321
Biomacromolecules 2016, 17, 215−224